



This is a repository copy of *Utilisation of molecularly imprinting technology for the detection of glucocorticoids for a point of care surface plasmon resonance (SPR) device.*

White Rose Research Online URL for this paper:

<https://eprints.whiterose.ac.uk/208454/>

Version: Published Version

---

**Article:**

Blackburn, C., Sullivan, M.V. [orcid.org/0000-0002-1771-8268](https://orcid.org/0000-0002-1771-8268), Wild, M.I. et al. (2 more authors) (2024) Utilisation of molecularly imprinting technology for the detection of glucocorticoids for a point of care surface plasmon resonance (SPR) device. *Analytica Chimica Acta*, 1285. 342004. ISSN 0003-2670

<https://doi.org/10.1016/j.aca.2023.342004>

---

**Reuse**

This article is distributed under the terms of the Creative Commons Attribution (CC BY) licence. This licence allows you to distribute, remix, tweak, and build upon the work, even commercially, as long as you credit the authors for the original work. More information and the full terms of the licence here:

<https://creativecommons.org/licenses/>

**Takedown**

If you consider content in White Rose Research Online to be in breach of UK law, please notify us by emailing [eprints@whiterose.ac.uk](mailto:eprints@whiterose.ac.uk) including the URL of the record and the reason for the withdrawal request.



[eprints@whiterose.ac.uk](mailto:eprints@whiterose.ac.uk)  
<https://eprints.whiterose.ac.uk/>



# Utilisation of molecularly imprinting technology for the detection of glucocorticoids for a point of care surface plasmon resonance (SPR) device

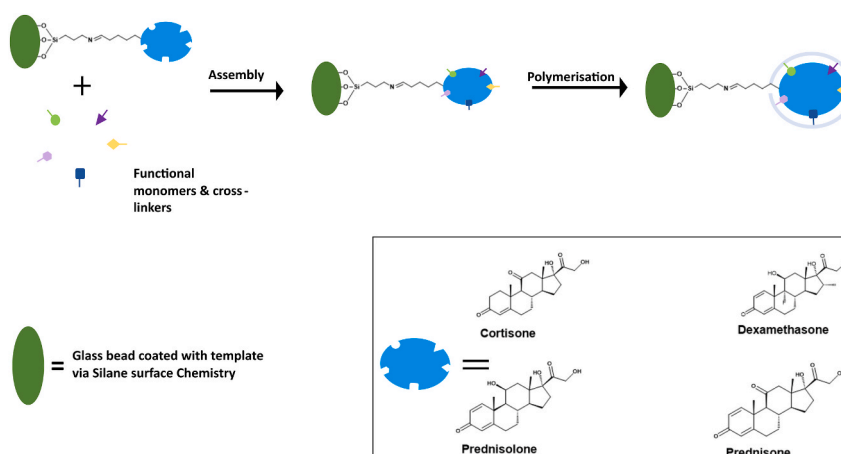
Chester Blackburn, Mark V. Sullivan, Molly I. Wild, Abbie J. O' Connor, Nicholas W. Turner\*

Department of Chemistry, University of Sheffield, Dainton Building, 13 Brook Hill, Sheffield, S3 7HF, UK

## HIGHLIGHTS

- The generation of four novel synthetic recognition nanomaterials via molecular imprinting technology.
- Affinity studies were performed, and materials displayed nanomolar affinities (15.9–62.8 nM) towards their target, with excellent selectivity.
- Theoretical LODs in both PBS and Surine™ were calculated and materials displayed very low limits of detection as a SPR sensing device (1.3–6.5 nM).
- These materials have the potential to replace chromatographic methods for the rapid detection of synthetic glucocorticoids in biological media.

## GRAPHICAL ABSTRACT



## ARTICLE INFO

Handling Editor: Prof Rebecca Lai

## ABSTRACT

Herein, we describe the synthesis and characterisation of four synthetic recognition materials (nanoMIPs) selective for the glucocorticoid steroids – prednisolone, prednisone, dexamethasone, and cortisone. Using a solid-phase synthesis approach, these materials were then applied in the development of a surface plasmon resonance (SPR) sensor for the detection of these four targets in doped urine, to mimic the routine testing of agricultural waste for possible environmental exposure. The synthesised particles displayed a range of sizes between 104 and 160 nm. Affinity studies were performed, and these synthetic materials were shown to display nanomolar affinities (15.9–62.8 nM) towards their desired targets. Furthermore, we conducted cross-reactivity studies to assess the materials selectivity towards their desired target and the materials showed excellent selectivity when compared to the non-desired target, with selectivity factors calculated. Furthermore, through the use of 3D visualisation it can be seen that small changes between structures (such as a hydroxyl to ketone transformation) there is excellent selectivity between the compounds in the ranges of 100 fold plus. Using Surine™ doped samples the materials offered comparable nanomolar affinities (10.7–75.7 nM) towards their targets when compared to the standardised buffer preparation. Detection levels in urine for all compounds was in the nanomolar range. The developed sensor offers potential for these devices to be used in the prevention of these

\* Corresponding author.

E-mail address: [n.w.turner@sheffield.ac.uk](mailto:n.w.turner@sheffield.ac.uk) (N.W. Turner).

<https://doi.org/10.1016/j.aca.2023.342004>

Received 26 September 2023; Received in revised form 3 November 2023; Accepted 4 November 2023

Available online 11 November 2023

0003-2670/Crown Copyright © 2023 Published by Elsevier B.V. This is an open access article under the CC BY license (<http://creativecommons.org/licenses/by/4.0/>).

pharmaceutical compounds to enter the surrounding environment through agricultural waste through monitoring at source. Likewise, they can be used to monitor use in clinical samples.

## 1. Introduction

Endocrine disruptors (EDs) are listed as pharmaceutical contaminants of emerging concern (CECs), and whilst most discussion is focused on sex hormones such as testosterone and estradiol glucocorticoid steroids are also becoming prevalent in nature [1,2]. Structurally, the glucocorticoid class of compounds generally consist of a tricyclic structure of cyclohexane and cyclopentane rings (Fig. 1) with molecular weights ranging between 300 and 400 Da. Additionally, the anti-inflammatory activity of this class of compounds has seen them in widespread use for a variety of different ailments, such as: asthma [3,4], arthritis [5] and inflammatory bowel disease (IBS) [6] for example. However, the incomplete removal of these compounds from pharmaceutical wastewater, sewage, agricultural and residential runoff presents a risk to both aquatic and terrestrial fauna that utilise these water sources [7,8].

Aquatically, the introduction of these substances generally stems from their use as a pharmaceutical. For the life that inhabit the water where their introduction occurs it has been reported that there have been adverse effects, especially in the fish populations [9–11].

Terrestrially, their use in animal husbandry has also been attributed to meat quality and quantity in veal and have been previously known to be administered illegally in tandem with anabolic steroids as growth promoters [12]. Furthermore, in veterinary science their use is not dissimilar to their use in human medicine, due to their anti-inflammatory properties [13,14]. Additionally, these substances are more likely to be found in the aqueous phase rather than in sludge or soil for example owing to, in general, their preference for this environment as suggested by their soil adsorption coefficient ( $K_{oc}$ ) and their n-octanol/water partition co-efficient ( $k_{ow}$ ) [15].

Currently, there are a variety of different methods for the detection

of glucocorticoids that have the potential to be released into the environment such as tandem liquid or gas chromatography coupled with mass spec (LC-MS/GC-MS) on animal faeces [16], urine [17] and wastewater [15,18]. For their use in humans numerous detection methods have been established due to their status as an illegal performance enhancing drugs, when administered by an oral, injectable or rectal route [19]. Nevertheless, detecting these compounds remains a time-consuming process, and, depending on hardware available and the form of the acquired sample, may require laborious steps before analysis can be performed. There has also been reported uses of glucocorticoid derivatives being detected via Enzyme-Linked Immunosorbant Assay (ELISA), however this technique has generally been made redundant by the advancements in chromatographic techniques that offer a much more sensitive platform. The current methods for detection of glucocorticoids (GCs) are summarised in Table 1.

Ideally, the opportunity to rapidly monitor urine sources *in situ* will allow for legal entities to be able to test on farm or slaughterhouse. Detecting the source compounds before they are released into the environment is advantageous as facilities can be well placed to ensure measures to limit their release into the environment [30].

Likewise, these compounds are vitally important in the clinical sphere. Monitoring of patients receiving systemic steroid therapy, for example in cases of asthma, is not new [31]. However, the users of such medication may present symptoms of disease such as Cushing syndrome [32] due to the side effects of using such medication. Therefore, to accurately quantify the root cause of cushingoid features, glucocorticoid screening may be performed with LC-MS as previously mentioned. However, as mentioned previously these methods are time consuming and may require laborious steps before analysis. Furthermore, acute and potentially life-threatening complications may arise from Cushing syndrome, for example cardiovascular complications [33]. Therefore, it is

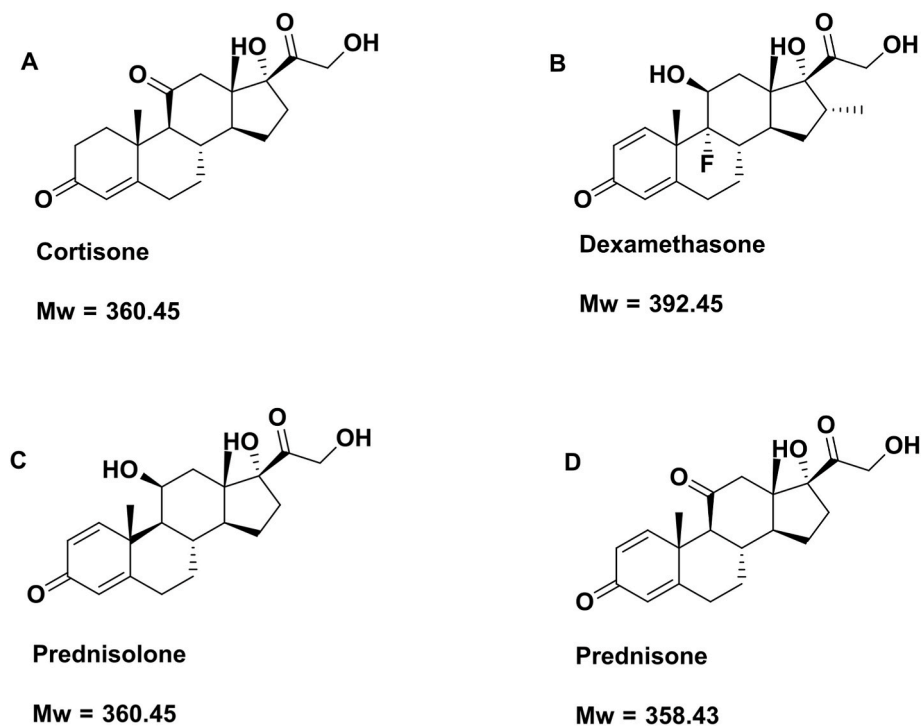


**Fig. 1.** The structures of: (A) Cortisone, (B) Dexamethasone, (C) Prednisolone, and (D) Prednisone – common glucocorticoids used in both therapeutic and agricultural settings.

**Table 1**  
Examples of available detection methods for glucocorticoid steroids.

Sample	Technique	Sample Prep <sup>a</sup>	Separation <sup>a</sup>	Detection <sup>a</sup>	Matrix	Sensitivity (LOD, LOQ)	Cross-Reactivity <sup>b</sup>	Reference
GCs	ELISA	–	–	–	Urine, Liver, Milk and Animal Feed	0.1 ppb (0.1 µg/L)	Dexamethasone (100%)	[20]
Betamethasone, Dexamethasone, Cortisone, Cortisol, Prednisone, Prednisolone	UHPLC-MS/MS	Filter 1.2 µm glass filter, filter 0.45 µm nylon, acidify to pH 2. SPE “pre-concentration” in MeOH (Oasis HLB sorbent)	Zorbax Eclipse XDB-C18. Solv A ternary mobile phase with a gradient elution Solvent A water/acetonitrile (78:22 v/v) with formic acid (0.1%) solvent B methanol/acetonitrile (78:22 v/v) with formic acid (0.1%). The gradient of 0.8% B increased to 5% in 5 min, 15% in 6.5 min, 50% in 0.5 min, kept constant for 1.5 min, increased to 99.9% in 0.5 min, kept constant for 0.5 min, and finally returned to 0.8% B in 0.5 min. 50 °C flow rate was 1 mL/min and the injection volume was 50 µL.	ESI -ve mode	River Water	Matrix dependant (0.5–7.5 ng/L)	–	[21]
GCs	LC-MS/MS	Filter samples with 1 µm glass filter, 1 L of surface water (2000:1 conc factor) or 500 mL of effluent (1000:1 conc factor). Spike with mix (1 ng). pH adjustment to pH 7.	MN Nuceloshell RP 18Plus column, 0.3 mL/min 10 µl injection volume. 25 °C	ESI + ve/-ve and ESI -ve	Wastewater effluent and surface water	Matrix Dependant Effluent (N/A, 0.02–0.5 ng/L) Surface Water (0.05–5 ng/L) (3–25 ng/L)	–	[22]
GCs	GC-MS	Extraction of samples from urine via SPE. Microwave assisted derivatization	Phenyl-methylsilicone column. He carrier gas 0.8 mL/min. Injection mode: 1:10, Injection volume 2 µl, 280 °C. Program 200 °C, 2 min, 15 C/min, final temp 300 °C 40 min, 20 °C/min final temp 320 °C 6 min, transfer line 290 °C.	EI	Urine sample, gaseous analyte		–	[23]
GCs	Ion mobility-high resolution mass spectrometry	1 mL of blank urine spiked with mixture of doping agent in water. Enzymatic hydrolysis and liquid-liquid extraction (10 fold pre-concentration)	UPLC oven 40 °C. Waters acquity UPLC BEH C18 column. Solvent A H <sub>2</sub> O and solvent B ACN with 0.1% formic acid. Gradient 2% B increasing to 98% B in 6 min. Decrease to 2% in 0.1 min follow by 4 min equilibrium. Flow rate 0.4 mL/min. Sample incubated on biosensor for 12 min and then EIS over 1 Hz to 10 kHz	ESI	Spiked urine sample	Analyte dependent, not explicitly specified	–	[24]
Cortisol	Electrochemical Impedance Spectroscopy (EIS)	Saliva filtered using polyvinylidene fluoride membrane. Centrifuge at 3500 rpm for 15 min.		Electrochemical	Human saliva	0.87 pM	–	[25]
Cortisol	Paper based microfluidic, screen printed electrode	Competitive assay of monoclonal antibody, AChE-labeled cortisol and cortisol	N/A	Electrochemical	PBS	10–140 ng/mL	–	[26]
Cortisol	Aptamer-functionalised nanoparticles – electrochemical device	Biological media spiked with known amount of target.	N/A	Electrochemical	Serum and Saliva	10 pg/mL	–	[27]
GCs	Poly(L-arginine)/ PSSA/QD modified sensor	Stand wastewater in fridge for 7 days and then collect supernatant. Filter with 0.45 µm filter. Dilute 100 fold with 0.1 mol/L CBS solution (pH 8).	N/A	Electrochemical	Wastewater	Analyte dependant 9–114 nm/L	–	[28]
GCs	Prism-Coupler MIP based	Targets spiked into biological medium of choice	N/A	Surface Plasmon Resonance	Urine, Plasma	5–11 ppb	–	[29]

<sup>a</sup> : applicable only to chromatographic techniques (LC and GC).

<sup>b</sup> : only applicable to ELISA technique.

vitaly important that a rapid, point of care device is available without the restrictions of pre-analytical work up, allowing the clinician to gain a rapid understanding of the patient's symptoms and assess whether glucocorticoid dosage requires tailoring for example.

In all the examples discussed above, the detection of levels of these synthetic steroids, is needed from complex matrices, and is beneficial at the point of analysis, rather than the need for lab testing. Thus, biosensor is a clear consideration.

Biological recognition bodies, such as antibodies are well known for their suitability of use in sensing devices due to their high affinity and excellent selectivity [34]. When utilised within a sensing device these biological recognition molecules offer a sensitive platform for detection with high selectivity towards the desired target [35]. However, this comes with drawbacks such as: inflated cost and they are time consuming to produce, sensitivity to environmental stimuli such as pH and temperature, short shelf life and in some cases the need for storage conditions which may be inaccessible to low GDP countries. These drawbacks have led to researchers to focus on synthetic recognition materials that can be used *in lieu* of their biological counterparts.

Molecularly imprinted polymers (MIPs) are synthetic recognition materials that have garnered both commercial and academic interest due to the potential of matching the performance of biological recognition molecules, without encountering the drawbacks previously mentioned [36,37]. The basic principles behind the MIP construction are simplistic whereby a template (target) molecule is complexed with functional monomers via non-covalent bonding such as Van-Der-Waals forces and hydrogen bonding [38]. These monomers are then polymerised entrapping the template in a highly cross-linked polymer network, after removal of this template molecule, the synthesised polymer retains cavities sterically and functionally complimentary to the extracted template, rebinding of this template is then facilitated through these formed cavities [39].

The progression of research into MIP technology has further led to the development of MIP nanoparticles (nanoMIPs) in which performance has been improved by the reduction in binding site heterogeneity and has opened the door for the possibility of these materials to take an active role in biological systems [40], as opposed to passive sensor systems. Furthermore, through the synthetic method developed for these nanomaterials there is a wider range of compatible templates than with a traditional bulk MIP for example. In addition, through the synthetic methods employed a 1:1 binding model can be used to easily model MIP recognition elements much like the modelling employed for their biological counterparts [41,42].

Surface Plasmon Resonance (SPR) is an optical sensor platform commonly employed to assess the affinity of biological recognition materials towards a specific ligand [43,44]. There have been a variety of different methodologies used to try and incorporate MIPs as the synthetic recognition material in SPR assays, through either thermal or electro-polymerisation onto the surface of the gold chip or, through click-chemistry to immobilise MIPs onto the surface of the chip bearing complimentary groups required for immobilisation (COOH for example). Due to the excellent sensitivity of the hardware and the capabilities to detect affinities in the nanomolar range SPR has seen itself rise to the forefront of researchers minds when it comes to sensor design and development [45,46].

Furthermore, SPR has the potential to be used in multiplexed detection systems, such as "eSPR" in which using an electrochemical flow cell the gold chip conventionally used for optical sensing can also act as a working electrode, generating both an optical and electrical signal for the detection of analytes. This method has been employed to obtain multidimensional data analytes such as H<sub>2</sub>O<sub>2</sub> [47], Immunoglobulin G [48] and the influenza virus [49] to name a few examples. Furthermore, other researchers have exploited the potential for SPR based imaging techniques namely "SPRi". For instance SPRi has been applied for a smartphone based biodetector [50] whilst also being applicable for high throughput screening of multiple analytes through

microarray technology [51,52] Additionally, there has been further work in fibre optic based SPR systems for the multiplexed detection of both PCR and affinity signals for applications such as DNA melt analysis [53].

Of course, such multiplexed systems offer numerous advantages against monomodal detection systems, as multiple signals can aid the researcher or clinician in achieving greater sensitivity in detection, whilst also offering corroborating data points. However, this can often come at a trade-off requiring more complex equipment due to the multiple signals/data streams being acquired and often higher operating costs due to the enhanced complexity of the systems overall. Furthermore, such systems require a much more technically adept operator, as thorough understanding of both methodologies being employed is required. Although this higher cost may in some cases be justified, in cases where such multiplexing is necessitated. This work synthesises nano-MIPs via the solid phase approach initially developed by the Piletsky group [54] and analysis was performed via Dynamic Light Scattering and Surface Plasmon Resonance. Once the performance of the polymer as a recognition material was ascertained, the sensor was exposed to doped Surine™ so that the performance at the point of possible exposure of these materials into the environment could be attained, whilst also confirming that the SPR based device can be used at the point of sample collection and no further derivatization or lab work up is required.

## 2. Experimental

### 2.1. Materials

Acrylic acid (AA), 3-aminopropyltrimethoxy-silane (APTMS), ammonium persulfate (APS), 1-Ethyl-3-(3-dimethylaminopropyl)carbodiimide (EDC), glutaraldehyde (GA), glycine, N-(3-aminopropyl)methacrylamide hydrochloride (NAPAm), *N,N'*-methylenebisacrylamide (BIS), *N*-hydroxysuccinimide (NHS), *N*-isopropylacrylamide (NIPAm), sodium dodecyl sulphate (SDS), *N*-*tert*-butylacrylamide (TBAm), and tetramethylethyldiamide (TEMED) were all purchased from Sigma-Aldrich (Poole, Dorset, UK).

Acetone, acetonitrile (dry), dipotassium phosphate, disodium phosphate, ethanolamine, ethylenediaminetetraacetic acid (EDTA), methanol, potassium chloride, sodium hydroxide, Tween 20 Cortisone, Dexamethasone, Prednisolone and Prednisone were all purchased from Fisher Scientific UK (Loughborough, Leicester, UK).

Glass beads (75 µm diameter) were purchased from Microbeads AG, (Brugg, Switzerland) and used as found.

Cerilliant Surine™ Negative Urine control was purchased from Merck, UK (Gillingham, Dorset)

All chemicals and solvents were analytical quality or high-performance liquid chromatography (HPLC) grade and were used as found without further purification.

### 2.2. Methodology

#### 2.2.1. Preparation of template-derivatized glass beads as affinity media

The preparation of the glass beads was as described in our prior work [55] Before template attachment, these were activated by boiling in 4 M NaOH (24 mL) for 15 min, washed with reverse-osmosis water (8 × 100 mL for 30 g of beads), until the resultant solution was pH 7. They were then subjected to 100 mL acetone wash and dried at 80 °C for 3 h.

The beads were placed into 12 mL solution of APTMS (3%, v/v) in anhydrous toluene for 24 h at 60 °C under a positive N<sub>2</sub> atmosphere, then further washed (8 × 100 mL acetone; 2 × 100 mL methanol). Finally, after draining, the beads were placed into an oven (150 °C for 30 min).

Afterwards, the beads that are now NH<sub>2</sub> surface functionalised were incubated in 15 mL of a 7% (v/v) aqueous solution of glutaraldehyde for 2 Hrs. The chosen template (either Cortisone, Dexamethasone,

Prednisolone or Prednisone) was then dissolved in 15 mL of a phosphate buffered saline solution (PBS, 10 mM, pH 7.4) and subsequently introduced to the glass beads and allowed to incubate overnight (16 Hrs) at room temperature (ca. 14 °C). The template derivatized beads were then filtered from solution and washed thoroughly with double distilled water (at least 1 L/10 × 100 mL washes) and dried. Afterwards, the beads were used immediately for the synthesis of the imprinted nano materials without further washing or characterization.

### 2.2.2. Solid-phase synthesis of glucocorticoid imprinted materials

Synthesis of the nanoMIPs was performed using a solid-phase method, scaled to 30 g of beads.

In summary, a 50 mL aqueous solution bearing 2.2 μL AA, 1 mg BIS, 7 mg NAPAm, 20 mg NIPAm, and 10 mg TBAm (dissolved prior in 250 μL ethanol) was generated. This was degassed via sparging with N<sub>2</sub> (20 min).

The 30 g of beads were placed in a 100 mL round bottom flask sealed with a rubber septum, which was purged with N<sub>2</sub> (10 min) before the addition of the polymerisation solution. To this mixture 12.5 μL TEMED and 15 mg APS dissolved in 250 μL were added to start the polymerisation reaction. The reaction was then swirled gently by hand and polymerisation was allowed to commence for 3 h at RT (ca. 14 °C) under a positive nitrogen environment.

To stop the reaction, the rubber septum was pierced exposing the mixture to the atmosphere and the beads were gravity filtered through 11 μm paper, and *in-situ* washed (8 × 30 mL water) at RT to removed unwanted materials and unused reactants. This step also washes off low affinity nanoMIPs. The beads were then collected and heated to 60 °C in 40 mL water then filtered through 11 μm paper with the filtrate collected. A series of water washes at 60 °C were carried out until approximately 150 mL of eluted high-affinity nanoparticles was collected. This solution was allowed to cool naturally to the ambient temperature, then stored at 4 °C (Fig. 2)

### 2.2.3. Characterization of nanoparticles

A 3 mL aliquot of the solution was oven-dried at 60 °C and the mass of the particles measured using a 6-point balance, allowing for a concentration (in μg mL<sup>-1</sup>) of the initial solution to be calculated. Particle size at 25 °C (effective hydrodynamic diameters (d<sub>h</sub>) was measured using dynamic light scattering (Brookhaven NanoBrook Omni

spectrometer using *Particle Solutions v 3.5*) with n = 6, in backscatter mode and CONTIN algorithm. Data was then exported, and graphs were reconstructed through OriginPro (OriginLab corporation, Northampton, USA)

Affinity and specificity of the imprinted nanoparticles for the different targets were studied using a Reichert 2 SPR system (Reichert Technologies, Buffalo, USA) with attached autosampler.

### 2.2.4. Immobilisation of NanoMIPs onto the SPR sensor surface

A carboxymethyl dextran hydrogel coated Au chip was preconditioned by a PBS pH 7.4 and 0.01 % Tween 20 running buffer (referred as PBST) at 10 μL min<sup>-1</sup> within the SPR. 1 mL of aqueous solution containing 40 mg EDC and 10 mg NHS was passed over the chip (6 min at 10 μL min<sup>-1</sup>).

300 μg of nanoMIPs in 1 mL of PBST and 10 mM sodium acetate, was injected over the left channel (working channel) of the chip for 1 min. The amine functionality of the nanoMIPs react with the functionalised surface leading to particle immobilisation. An 8-min injection over both channels (working and reference) of quenching solution (1 M ethanolamine, pH 8.5) was added; to “cap” any unreacted dextran on the surface followed by a continuous flow of PBST at 10 μL min<sup>-1</sup>. All injections were taken from a stable baseline.

### 2.2.5. Kinetic analysis using SPR

Kinetic analysis in rebinding of analyte (target and cross-reactivity) to the nanoMIP was performed in set pattern of 2-min association (PBST with analyte concentrations 4, 16, 32, 64 nM), 5-min dissociation (PBST only) and a regeneration cycle (regeneration buffer 10 mM Glycine-HCl, pH 2 for 1 min) followed by a final stabilisation cycle (PBST for 1 min). An initial injection of blank PBST was used as the first run with increasing analyte concentration for subsequent runs. After the analyses were completed, signals from reference channel were subtracted from signals from the working. In all cases rebinding was studied in triplicate.

The SPR responses were fitted to a 1:1 Langmuir fit bio-interaction (BI) model using the Reichert *TraceDrawer* software. Association rate constants (k<sub>a</sub>), dissociation rate constants (k<sub>d</sub>), and maximum binding (B<sub>max</sub>) were fitted globally, whereas the BI signal was fitted locally. Equilibrium dissociation constants (K<sub>D</sub>) were calculated by k<sub>d</sub>/k<sub>a</sub>. For each nanoMIP/analyte combination a calibration curve was generated

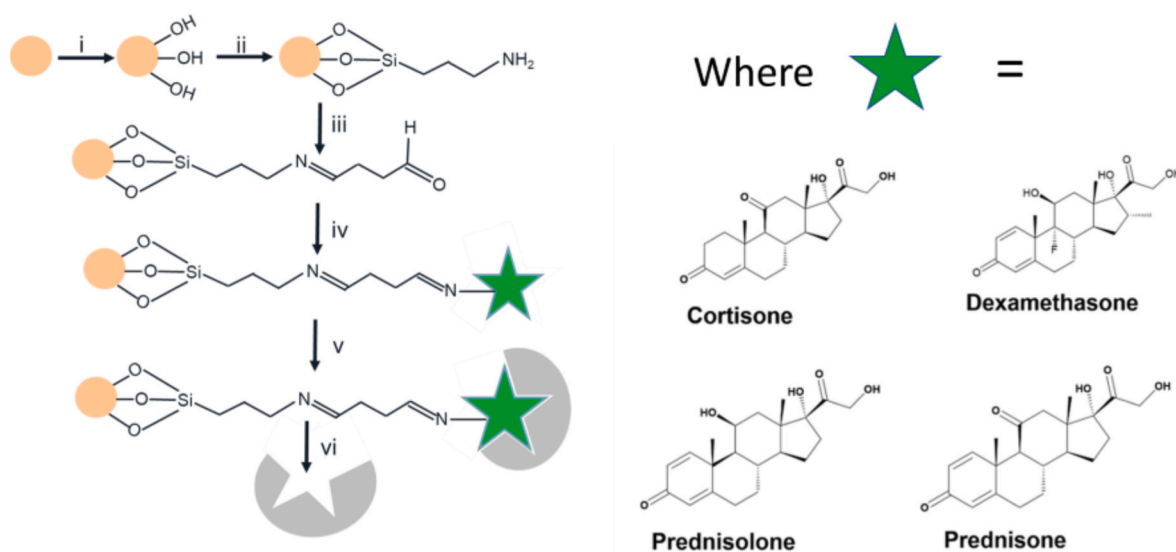


Fig. 2. Representative cartoon schematic of solid phase synthesis of nanoMIPs. i. Addition of hydroxy groups to silica bead. ii. Addition of amino silane – functionalisation. iii. Addition of linking group (e.g. glutaraldehyde). iv. Addition of template (epitope, drug, protein etc) v: Build imprinted polymeric scaffold around the template (addition of monomer mixture) vi: Cold wash removes low-affinity materials followed by hot wash to realise nanomaterials.

across the concentration 4 nM–64 nM taking  $n = 3$  average. From this, a theoretical LOD was calculated. Where signal saturation was observed a natural logarithmic trendline was applied for the calculation.

### 3. Results and discussion

#### 3.1. MIP synthesis and particle size

Using a solid-phase suspension polymerisation approach imprinted recognition materials were produced utilising an adapted methodology based composition and reaction conditions suggested by Canfarotta et al. [41,42,54]. The synthetic recognition materials (nanoMIPs) were synthesised for the target glucocorticoids: prednisolone, prednisone, dexamethasone and cortisone. The incorporation of stimuli responsive NIPAm [56] in the polymer chain allows for relatively simple removal of the material post polymerisation, using a hot wash, whilst also affording maintenance of site structure and imprinted cavities.

The concentrations of nanoMIPs for the glucocorticoids alongside particle size assessments can be found in Table 1. Briefly, post polymerisation a 150 mL sample of nanoMIPs is recovered, we deduce the concentration of this solution by drying a 3 mL aliquot ( $n = 3$ ) and from this concentration our overall yield of material can be inferred. For analysis, generally around 1 mg of material will suffice for both SPR (300  $\mu\text{g}$  per chip) and DLS (ca. 100  $\mu\text{g mL}^{-1}$ ), hence the expected yield from our synthesis is more than sufficient for these studies. While this is consistent with our previous work [41,42], we are actively researching methods to further improve this yield, without negative implications to the synthetic recognition material.

The nanomaterials were characterised via Dynamic Light Scattering, where aggregation of the nanoMIPs (within 20 s) was discovered and as such the data obtained via intensity of scattered light was converted into number distribution to negate the aggregation effects. These are presented in Table 2 and are in good agreement with one another. Furthermore, the size distribution graphs can be found in the supplementary information (Fig. S1) where aggregation can be clearly seen and that through transformation the nanoMIPs can be much more readily visualised.

#### 3.2. $K_D$ affinity measurements and sensor performance

The incorporation of amine functionality within the nanoMIP polymer scaffold allows for conventional click chemistry via NHS/EDC Steglich-type esterification [57,58]. This allows for covalent linkage of the nanoMIPs to the surface of a SPR chip was facilitated through this chemistry, with the SPR chips used in this study composed of carboxymethyl dextran hydrogel coated gold. Thus, presenting  $-\text{COOH}$  on the surface of the chip and allowing for the relatively simple and well understood Steglich-type reaction to proceed [57]. Additionally, the use of ethanolamine post immobilisation allowed for any residual functionality on the surface of the SPR chip to be “capped” thus, preventing subsequent reactions during the kinetic studies, removing the potential for false recognition readings.

Using this workflow, a monolayer of recognition material is expected to be deposited on top of the SPR chip, as the nanoMIP functionality

**Table 2**

Calculated concentration and particle size for the glucocorticoids imprinted nanoparticles (nanoMIPs). All experiments were performed under ambient conditions. Number of repeats = 3.

Template	Concentration ( $\mu\text{g mL}^{-1}$ )	Diameter Intensity (nm)	Diameter Number (nm)
Prednisolone	120 ( $\pm 20$ )	104 ( $\pm 4$ )	104 ( $\pm 5$ )
Prednisone	130 ( $\pm 27$ )	160 ( $\pm 12$ )	160 ( $\pm 12$ )
Dexamethasone	100 ( $\pm 30$ )	127 ( $\pm 6$ )	126 ( $\pm 9$ )
Cortisone	190 ( $\pm 3$ )	133 ( $\pm 14$ )	133 ( $\pm 14$ )

dictates, through design, they are inclined to react and link with the activated  $-\text{COOH}$  groups on the surface of the chip as opposed to reacting with themselves. The nanoMIP material is flowed across the chip in an excess, to ensure that maximum coverage on the chip surface is obtained. All immobilisation curves can be found labeled with the appropriate stage of the surface functionalisation in the supplementary information (Fig. S2)

Furthermore, by having maximum receptor (binding population) allows for standard models for ligand/receptor interactions to be applied and as such a 1:1 kinetic model can be used for ligand/receptor interactions. Given the nature of the imprinting process this is a widely accepted model for their analysis and allows for comparisons be drawn towards their biological counterparts.

SPR is not the only optical sensing technology that can be employed today, however. Other methodologies such as electrochemiluminescence and photonic crystal devices could be considered for the detection of these molecules, as a label free technique comparable to the use of SPR described in this paper.

However, due to the lack of fluorescent activity of the steroid's fluorescence-based sensing could not be used in a comparable label free technique. Additionally, due to protein content in the surine, the matrix itself would induce interference that would lend fluorescence-based techniques redundant, or at the very least extremely cumbersome and time consuming.

An excellent alternative device would be the use of a photonic crystal device for the detection of these molecules, with the integration of template specific nanoMIPs incorporated into the sensing device itself. However, further work is required in the field of photonic crystals before these can become a reliable alternative, at least in the two- and three-dimensional space. Regarding crystals in just one-dimension high sensitivity and stability can be afforded [59–62]. Indeed, it is because of these properties that researchers have begun work fabricating photonic crystal sensors utilising SPR technology [63–65]. This is something that is worth considering, however a great deal of work is required in the space of molecular imprinting before MIPs may be used in such a device [66].

A further consideration would be the use of quantum dot (QD) technology. QDs have been used within SPR technology before, due to their excellent optical properties are prime candidates for the amplification of signals, such as from antibodies for example [67]. However, despite the advantages these nanomaterials offer, they are applied in this space as a label. Therefore, in this work quantum dot technology has been omitted, as the scope of the work was to produce a label free biosensor that could be used readily and rapidly with a raw sample, with little to no work up required.

Additionally, it must be noted that the benefits of SPR technology are that a MIP can be readily immobilised onto a gold slide and through proper regeneration and removal of the template can be used repeatedly, reducing cost. It must be stated that within this work each chip underwent at least 15 cycles of rebinding and regeneration with no observed degradation, suggesting a robust, reusable, and cost-efficient approach to sensing. For these reasons and the reasons discussed above therefore an SPR based sensor was decided upon as the most appropriate application for these nanoMIPs.

The nanoMIP immobilised SPR chips (MIP-Chips) were then used in a series rebinding and selectivity studies for the corresponding target and non-target glucocorticoids.

The solid phase synthesis approach was chosen against bulk or hydrogel type MIPs for numerous reasons for example, MIP is removed from template and is facilitated via a hot wash in which the intermolecular forces and pure nanoMIPs can be collected relatively easily, and without the need for grinding (as seen in bulk MIPs) or sieving (as seen in hydrogel MIPs) providing a facile approach to synthesis of recognition agents, whilst maintaining homogeneity. Furthermore, the analytical instrument of choice was a SPR machine, and the penetration depth of the laser is estimated to be around 400 nm, therefore, it is imperative

that a nanoMIP was synthesised, the solid phase approach consistently yields nanoMIPs, that are appropriate for this technique.

The SPR sensorgraphs presented in Fig. 3, show the interactions with the five different interactions of the target glucocorticoids (Cortisone, dexamethasone, prednisolone, and prednisone), with their corresponding nanoMIPs (Fig. 2A, B, C, and D, respectively), immobilised onto the surface of the gold SPR chip surface. From these curves and application of the 1:1 kinetic model we can deduce and overall equilibrium dissociation constant ( $K_D$ ) for the targets interacting with their nanoMIPs (Table 3).

The recognition of the imprinted nanomaterials with the glucocorticoid molecules and their corresponding nanoMIPs were calculated with the  $K_D$  values shown to be 15.9 nM, 24.9 nM, 62.8 nM, and 29.7 nM for the Cortisone, Dexamethasone, Prednisolone, and Prednisone nanoMIPs, respectively. These nanomolar values are consistent with those of other nanoMIPs, imprinted for similarly small molecular weight targets [68]. Our previous work producing nanoMIPs imprinted for SARMS molecules and antibiotic targets also produced  $K_D$  values within the nanomolar range [41,42].

To explore the specific recognition and selectivity of the imprinted nanomaterial, cross-reactivity was studied by loading non-target glucocorticoid molecules onto the nanoMIP SPR gold chip. The affinity towards the non-targets is represent in Table 3, with the dissociation constants ( $K_D$  values) shown and the corresponding SPR curves presented in Figs. S3–S6. Dexamethasone, Prednisolone and Prednisone was used to evaluate the Cortisone nanoMIP (Fig. S3), Cortisone, Prednisolone and Prednisone was used to test the Dexamethasone nanoMIP (Fig. S4), Cortisone Dexamethasone, and Prednisone was used to test the Prednisolone nanoMIP (Fig. S5), and Cortisone Dexamethasone, and Prednisolone was used to test the Prednisone nanoMIP (Fig. S6). All experiments were performed in triplicate with an average produced and with the  $K_D$  values for the non-target glucocorticoid molecules interacting with the nanoMIPs estimated via the *TraceDrawer* software, presented in Table 3. Furthermore, the selectivity factor of the materials can be found in Table 4 and towards their true target the nanoMIPs are highly selective. The use of the SF was decided up as the use of a non-imprinted polymer (NIP) is traditionally used as a control to generate an imprinting factor (IF). This factor is used to measure the strength of interactions of a target towards MIP [69]. However, it is

**Table 3**

Calculated equilibrium dissociation constants ( $K_D$ ) of the nanoMIPs from the data presented in Fig. 2 and S2-5. All experiments were performed under ambient conditions. Number of repeats = 3.

	$K_D$ (nM)			
	Cortisone	Dexamethasone	Prednisolone	Prednisone
Cortisone nanoMIP	15.9 ( ± 0.5)	7600 (±380)	8040 (±760)	6020 (±540)
Dexamethasone nanoMIP	2580 (±270)	24.9 ( ± 1.6)	6980 (±390)	1670 (±20)
Prednisolone nanoMIP	8530 (±600)	6430 (±410)	62.8 ( ± 4.3)	8090 (±570)
Prednisone nanoMIP	2280 (±40)	7440 (±470)	4430 (±240)	29.7 ( ± 1.7)

**Table 4**

Calculated Selectivity Factors (SF) of the nanoMIPs from the data presented in Fig. 2 and S2-5. All experiments were performed under ambient conditions. Number of repeats = 3.

	Selectivity Factor (SF)			
	Cortisone	Dexamethasone	Prednisolone	Prednisone
Cortisone nanoMIP	—	478	506	379
Dexamethasone nanoMIP	104	—	280	67
Prednisolone nanoMIP	136	102	—	129
Prednisone nanoMIP	77	250	149	—

widely accepted that the use of a selectivity factor (SF) gives a better indication of the binding ability of a MIP towards their desired target [70–72]. The recent development of the nanoMIP technology in 2016, via a solid phase synthesis approach requires a nucleation site, in this case a covalently affixed template to glass bead, for the synthesis of such recognition materials to proceed. However, because of this the synthesis of a NIP is not possible in the same way [54,68], due to this both NIP and IF are redundant in this study. Therefore, through cross reactivity and selectivity factors the selectivity of these synthesised nanoMIPs has been quantified.

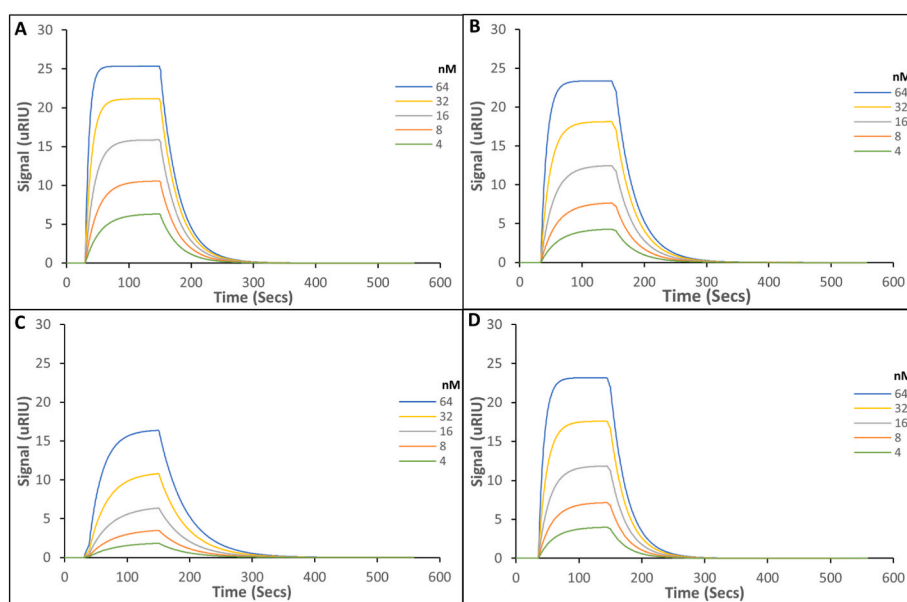


**Fig. 3.** Representative SPR curves showing rebinding of the target glucocorticoids to their corresponding immobilised nanoMIPs. Five concentrations of analyte in PBST. (A) Cortisone binding to Cortisone-imprinted nanoMIPs; (B) Dexamethasone binding to Dexamethasone-imprinted nanoMIP, (C) Prednisolone binding to Prednisolone-imprinted nanoMIP, and (D) Prednisone binding to Prednisone-imprinted nanoMIP.

These values were calculated using the following formula (eq. 1).

$$(eq.1) SF = \frac{\text{affinity of target}}{\text{affinity of nontarget}}$$

When the nanoMIPs were loaded with non-target molecules, recognition significantly decreased with  $K_D$  values observed in the  $\mu\text{M}$  range, demonstrating target specificity towards their desired target with the Cortisone nanoMIP displaying the best selectivity. Furthermore, to showcase the power of the imprinting process and the selectivity the technique affords, we have 3D modelled the target molecules in BIOVIA Discovery Studio so that the steric effects the MIP recognises can be appreciated. It is shown through this modelling that the oxidation of the prednisolone hydroxyl into a ketone and the reduction of the double bond present in cortisone into a more flexible alkane in prednisone effects the selectivity of the MIP significantly, thus showcasing the power of the technique as no derivatization was required pre-analysis (Fig. 4).

Furthermore, we have calculated theoretical limits of detection for the nanoMIP sensors, however, due to high saturation the data points observed displayed a logarithmic trend (Supplementary Information Fig. S7). This is common in complex matrices such as these. There is potential for pre-clean-up of the sample in question to attempt to alleviate these issues however, this was beyond the scope of this study, in which the aims were to produce a synthetic recognition agent capable of performing as a selective sensor. Therefore, by using a natural logarithmic trendline for the calculations it is shown that during our experiments we were working close to the theoretical limit of detection, but never below, giving further confidence in the obtained  $K_D$  values. The values obtained from the calculations can be seen in Table 5.

The glucocorticoid molecules used with this study are widely used for the treatment of inflammation, autoimmune diseases, and cancer, amongst others, and as such long-term use could cause significant health problems [73]. As such, there is a necessary requirement for being able to demonstrate detection of these molecules within biological matrices.

**Table 5**

Theoretical LODs for nanoMIPs loaded with their desired target in PBST.

NanoMIP	Theoretical LOD (nM)
Cortisone	1.6
Dexamethasone	2.4
Prednisolone	3.6
Prednisone	2.6

Therefore, detection from a synthetic urine was explored as a mimic for testing urine samples. Surine™ was spiked with the target analytes at concentrations between 4 and 64 nM and tested with the modified sensor surface.

Fig. 5 shows the representative SPR curves for the interactions of the glucocorticoid molecules in Surine™, and their corresponding nanoMIP loaded SPR sensor chip, with the equilibrium dissociation constant ( $K_D$ ) for the targets shown in Table 3.

When compared with the data in Figs. 3 and 5 shows a noticeable difference with the overall size of the signal intensity. This is due to a significant matrix effect within the sample that is observed and is to be expected especially with the substantial differences in the density and optical properties of the Surine™ and PBST. This is a frequent experience, and a known architect of SPR which utilises optical phenomenon to monitor changes in refractive index and has also been seen in our previous work using spike foetal calf serum, spiked milk, and spiked river water samples [41,42].

The  $K_D$  values shown in Table 6, are consistent with those shown in Table 3, 15.9, 24.9, 62.8, and 29.7 nM, compared with 10.7, 45.6, 75.7, 59.0 nM for Cortisone, Dexamethasone, Prednisolone, Prednisone nanoMIPs, respectively. These slight differences in  $K_D$  values are to be expected, especially given the differences in optical effects caused by the changes in the matrices and environments between samples dissolved in

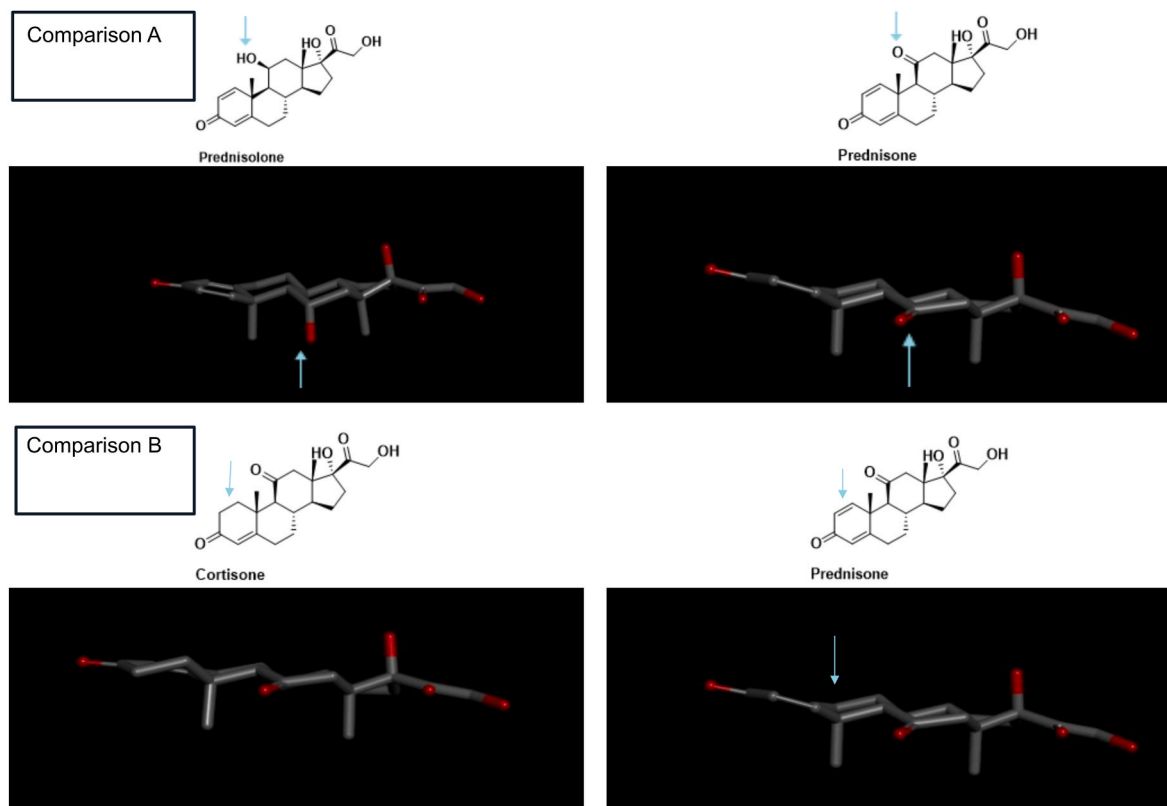


**Fig. 4.** 3D representation of steroid targets in lowest energy conformation via BIOVIA Discovery Studio, showing chemical and structural changes between the similar structures affording the selectivity of the NanoMIPs. Comparison A: Prednisolone vs Prednisone and Comparison B: Cortisone vs Prednisone.

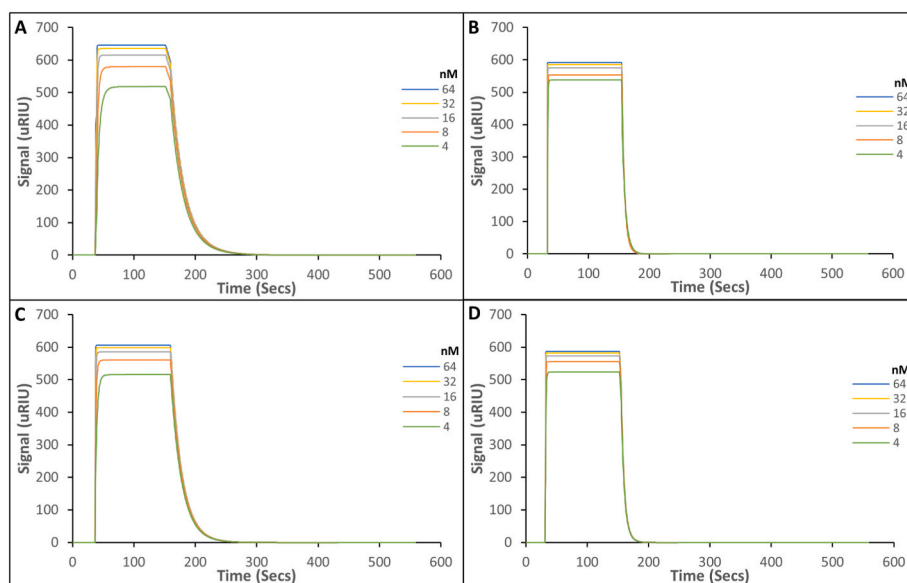


**Fig. 5.** Representative SPR curves showing rebinding of the target glucocorticoids to their corresponding immobilised nanoMIPs. Five concentrations of analyte in Surine™. (A) Cortisone binding to Cortisone-imprinted nanoMIPs; (B) Dexamethasone binding to Dexamethasone-imprinted nanoMIP, (C) Prednisolone binding to Prednisolone-imprinted nanoMIP, and Prednisone binding to Prednisone-imprinted nanoMIP.

**Table 6**

Calculated equilibrium dissociation constants ( $K_D$ ) of the target analytes binding to their corresponding nanoMIPs, from Surine™ using the data presented in Fig. 5. All experiments were performed under ambient conditions. Number of repeats = 3.

	$K_D$ (nM)
	Target reloaded from spiked Surine™
Cortisone nanoMIP	10.7 ( $\pm 1.3$ )
Dexamethasone nanoMIP	45.6 ( $\pm 3.0$ )
Prednisolone nanoMIP	75.7 ( $\pm 5.3$ )
Prednisone nanoMIP	59.0 ( $\pm 5.7$ )

**Table 7**

Theoretical LODs for nanoMIPs loaded with their desired target in Surine.

NanoMIP	Theoretical LOD (nM)
Cortisone	1.76
Dexamethasone	0.52
Prednisolone	0.56
Prednisone	1.61

PBST compared with Surine™, in terms of pH, ionic strength *etc.*, all of which will affect binding interactions. With the data shows that the detection of glucocorticoid molecules is possible from biological samples (Surine™) using a synthetic recognition material (nanoMIP). Table 5 displays the theoretical LODs of the desired targets in the Surine™ media in which the same method, as previously used for PBST LODs, was used due to high saturation of the samples (the urine sample has a significantly different optical density to the PBST, which affects the signal obtained by the SPR) a natural logarithmic curve was obtained (Fig. S8) (see Table 7).

#### 4. Conclusions and future direction

This work highlights the developments and benefits of molecularly imprinted nanoMIP technology in the design and creation of synthetic recognition materials, and their subsequent advantages over biological counterparts. Four different glucocorticoid steroids were used as

molecules of interest as templates to demonstrate the effectiveness for the imprinting process, utilising the benefits of a solid-phase synthetic approach. This method further demonstrates that  $K_D$  values ranging from 15 to 63 nM are achievable using this nanoMIP approach, thus showing that the production of high functioning synthetic recognition materials that can produce biological level recognition, but with the added benefit of custom design and resistance to extremes of pH and temperature.

Using SPR as a sensing apparatus we have shown that there is no need for derivatization or hydrolysis of these compounds as required in other methodologies for glucocorticoid testing, such as GC-MS and LC-MS. Furthermore, whilst this current research highlights the advantages of these materials as a recognition element for sensing, we are interested and look to study the engineering of devices, such as membrane filters so that imprinted materials can offer more cost benefit to the end users, through both sensing applications and removal and remedial applications, such as water treatment.

However, there have been some drawbacks observed that must be noted. Firstly, due to saturation effects observed in Surine, it is suggested that calibration curves are prepared for these complex matrices each time a new matrix is used, which can be time consuming. Furthermore, biofouling can affect the sensor's response. Additionally, whilst derivatization is not required, there may be a need for a pre-work up step on the sample itself, such as dilutions to mitigate the effects of saturation on the nanoMIPs. Finally, this work has not been produced at a commercial scale (1 Kg+) and therefore, the effects of such scale up on both the nanoMIP itself and batch to batch variability is not well understood. Our studies in this are continue and we are exploring ways to improve the sensor performance, especially around sample preparation.

The particle size range does highlight some key queries within the imprinting process however, despite consistent sizes throughout the study, we have seen variations in ours and other researchers' studies depending on the template used. We are actively looking at methodologies and optimisations that will both reduce time needed to synthesise these materials, whilst also affording control over the final particle size of the materials. It is believed that through the control of the size of the particle itself, we would be able to fine tune these recognition materials, to better optimise the synthetic process to suit variations in template.

## CRedit authorship contribution statement

**Chester Blackburn:** Investigation, characterisation, data, Formal analysis, Writing – original draft, Writing – review & editing, All authors have read and agreed to the published version of the manuscript. contributed equally to this work. **Mark V. Sullivan:** characterisation, data, Formal analysis, Writing – original draft, Writing – review & editing, All authors have read and agreed to the published version of the manuscript. contributed equally to this work. **Molly I. Wild:** Investigation, data, Formal analysis, All authors have read and agreed to the published version of the manuscript. **Abbie J. O' Connor:** Investigation, All authors have read and agreed to the published version of the manuscript. **Nicholas W. Turner:** Grant, acquisition, Conceptualization, Formal analysis, Writing – original draft, Writing – review & editing, All authors have read and agreed to the published version of the manuscript.

## Declaration of competing interest

On Behalf of Professor Turner and his group, I have the pleasure of submitting our manuscript entitled "Utilisation of Molecularly Imprinting Technology for the Detection of Glucocorticoids for a Point of Care Surface Plasmon Resonance (SPR) Device" for publication in your journal. We believe that this manuscript is appropriate for publication by *Analytica Chimica Acta* because our work encompasses an optical sensing device incorporating a biomimetic recognition device.

Thank you for your consideration of this manuscript and we look forward to your response. We have no conflicts of interest to disclose.

## Data availability

Data will be made available on request.

## Acknowledgements

This work was partly funded by University of Sheffield postgraduate budgets and EPSRC grant EP/V056085/2.

## Appendix A. Supplementary data

Supplementary data to this article can be found online at <https://doi.org/10.1016/j.aca.2023.342004>.

## References

- M.I. Llamas-Dios, I. Vadillo, P. Jiménez-Gavilán, L. Candela, C. Corada-Fernández, *Sci. Total Environ.* 788 (2021), 147822.
- S. Sauvé, M. Desrosiers, *Chem. Cent. J.* 8 (2014) 15.
- R.J. Freishtat, K. Nagaraju, W. Jusko, E.P. Hoffman, *J. Invest. Med.* 58 (2010) 19–22.
- V.H.J. Van Der Velden, *Mediat. Inflamm.* 7 (1998) 229–237.
- C. Hua, F. Buttgerit, B. Combe, *RMD Open* 6 (2020) 1–9.
- S. Bruscoli, M. Febo, C. Riccardi, G. Migliorati, *Front. Immunol.* 12 (2021) 1–9.
- J. Gong, C. Lin, X. Xiong, D. Chen, Y. Chen, Y. Zhou, C. Wu, Y. Du, *Environ. Pollut.* 251 (2019) 102–109.
- C.M. Hamilton, M.J. Winter, L. Margiotta-Casaluci, S.F. Owen, C.R. Tyler, *Environ. Int.* 162 (2022), 107163.
- C.A. Lalone, D.L. Villeneuve, A.W. Olmstead, E.K. Medlock, M.D. Kahl, K. M. Jensen, E.J. Durhan, E.A. Makynen, C.A. Blanksma, J.E. Cavallin, L.M. Thomas, S.M. Seidl, S.Y. Skolness, L.C. Wehmas, R.D. Johnson, G.T. Ankley, *Environ. Toxicol. Chem.* 31 (2012) 611–622.
- L. Margiotta-Casaluci, S.F. Owen, B. Huerta, S. Rodríguez-Mozaz, S. Kugathas, D. Barceló, M. Rand-Weaver, J.P. Sumpter, *Sci. Rep.* 6 (2016) 1–13.
- R.A. Willi, S. Faltermann, T. Hettich, K. Fent, *Environ. Sci. Technol.* 52 (2018) 877–885.
- M. Tarantola, A. Schiavone, G. Preziuso, C. Russo, B. Biolatti, D. Bergero, *Anim. Sci.* 79 (2004) 93–98.
- D. O'Neill, A. Hendricks, J. Summers, D. Brodbelt, *J. Small Anim. Pract.* 53 (2012) 217–222.
- M.A. Aharon, J.E. Prittie, K. Buriko, *J. Vet. Emerg. Crit. Care* 27 (2017) 267–277.
- S. Liu, G.G. Ying, J.L. Zhao, L.J. Zhou, B. Yang, Z.F. Chen, H.J. Lai, *J. Environ. Monit.* 14 (2012) 482–491.
- N. De Clercq, J. Vanden Bussche, S. Croubels, P. Delahaut, L. Vanhaecke, *J. Chromatogr. A* 1336 (2014) 76–86.
- J.P. Antignac, B. Le Bizec, F. Monteau, F. André, *Steroids* 67 (2002) 873–882.
- E.M. Driver, A.J. Gushgari, J.C. Steele, D.A. Bowes, R.U. Halden, *Sci. Total Environ.* 838 (2022), 155961.
- WADA Banned substances list, <https://www.wada-ama.org/en/prohibited-list>, (accessed 26 April 2023).
- T. Shibata, R. Hasegawa, K. Mochida, *Yakugaku Zasshi J. Pharm. Soc. Japan* 103 (1983) 1054–1059.
- P. Herrero, F. Borrull, E. Pocurull, R.M. Marcé, *J. Chromatogr. A* 1224 (2012) 19–26.
- A. Weizel, M.P. Schlüsener, G. Dierkes, T.A. Ternes, *Environ. Sci. Technol.* 52 (2018) 5296–5307.
- L. Amendola, F. Garribba, F. Botre, *Anal. Chim. Acta* 489 (2003) 233–243.
- K. Plachká, J. Pezzatti, A. Musenga, R. Nicoli, T. Kuranne, S. Rudaz, L. Nováková, D. Guillarme, *Anal. Chim. Acta* 1175 (2021), 338739.
- M.S. Khan, K. Dighe, Z. Wang, I. Srivastava, A.S. Schwartz-Duval, S.K. Misra, *D. Pan, Analyst* 144 (2019) 1448–1457.
- L. Fiore, V. Mazzaracchio, A. Serani, G. Fabiani, L. Fabiani, G. Volpe, D. Moscone, G.M. Bianco, C. Occhiuzzi, G. Marrocco, *Sensor. Actuator. B Chem.* 379 (2023), 133258.
- B.J. Sanghavi, J.A. Moore, J.L. Chávez, J.A. Hagen, N. Kelley-Loughnane, C.-F. Chou, N.S. Swami, *Biosens. Bioelectron.* 78 (2016) 244–252.
- Z. Luo, N. He, X. Chen, L. Yu, Y. Ma, X. Cui, J. Xu, A. Zeng, *J. Electrochem. Soc.* 169 (2022), 77516.
- E. Sari, R. Üzek, M. Duman, H.Y. Alagöz, A. Denizli, *Sensor. Actuator. B Chem.* 260 (2018) 432–444.
- J.O. Ojogoro, M.D. Scrimshaw, J.P. Sumpter, *Sci. Total Environ.* 792 (2021), 148306.
- L. Fardet, I. Petersen, I. Nazareth, *Med. (United States)* 94 (2015) 1–10.
- S. Manubolu, O. Nwosu, *J. Clin. Transl. Endocrinol. Case Reports* 6 (2017) 4–8.
- M.H. Scherthauer-Reiter, C. Siess, A. Micko, C. Zauner, S. Wolfsberger, C. Scheuba, P. Riss, E. Knosp, A. Kautzky-Willer, A. Luger, G. Vila, *J. Clin. Endocrinol. Metab.* 106 (2021) E2035–E2046.
- M.A. Morales, J.M. Halpern, *Bioconjug. Chem.* 29 (2018) 3231–3239.
- T.R.J. Holford, F. Davis, S.P.J. Higson, *Biosens. Bioelectron.* 34 (2012) 12–24.
- K. Mosbach, O. Ramstrom, *Nat. Biotechnol.* 14 (1996) 163–170.
- M. V Sullivan, W.J. Stockburn, P.C. Hawes, *Nanotechnology* 32 (2021), 095502.
- N.W. Turner, C.W. Jeans, K.R. Brain, C.J. Allender, V. Hlady, D.W. Britt, *Biotechnol. Prog.* 22 (2006) 1474–1489.
- P.S. Sharma, Z. Iskierko, A. Pietrzyk-Le, F. D'Souza, W. Kutner, *Electrochem. Commun.* 50 (2015) 81–87.
- S.A. Piletsky, T.S. Bedwell, R. Paoletti, K. Karim, F. Canfarotta, R. Norman, D.J. L. Jones, N.W. Turner, E.V. Piletska, *J. Mater. Chem. B* 10 (2022) 6732–6741.
- A. Henderson, M. V Sullivan, R.A. Hand, N.W. Turner, *J. Mater. Chem. B* 10 (2022) 6792–6799.
- M. V Sullivan, A. Henderson, R.A. Hand, N.W. Turner, *Anal. Bioanal. Chem.* 414 (2022) 3687–3696.
- Y. Tang, X. Zeng, J. Liang, *J. Chem. Educ.* 87 (2010) 742–746.
- S. Firdous, S. Anwar, R. Rafya, *Laser Phys. Lett.* 15 (2018), 65602.
- F. Fernandez, D.G. Pinacho, F. Sanchez-Baeza, M.P. Marco, *J. Agric. Food Chem.* 59 (2011) 5036–5043.
- S.M. Derayea, M.A. Omara, M.A. Hammada, Y.F. Hassanb, *J. Appl. Pharmaceut. Sci.* 7 (2017) 16–24.
- Y. Mao, Y. Bao, W. Wang, Z. Li, F. Li, L. Niu, *Talanta* 85 (2011) 2106–2112.
- S. Sriwichai, A. Baba, S. Phanichphant, K. Shinbo, K. Kato, F. Kaneko, *Sensor. Actuator. B Chem.* 147 (2010) 322–329.
- A.H. Qatamin, J.H. Ghithan, M. Moreno, B.M. Nunn, K.B. Jones, F.P. Zamborini, R. S. Keynton, M.G. O'Toole, S.B. Mendes, *Appl. Opt.* 58 (2019) 2839.
- H. Guner, E. Ozgur, G. Kokturk, M. Celik, E. Esen, A.E. Topal, S. Ayas, Y. Uludag, C. Elbuken, A. Dana, *Sensor. Actuator. B Chem.* 239 (2017) 571–577.
- J.B. Fasoli, R.M. Corn, *Langmuir* 31 (2015) 9527–9536.
- C.L. Wong, G.C.K. Chen, X. Li, B.K. Ng, P. Shum, P. Chen, Z. Lin, C. Lin, M. Olivo, *Biosens. Bioelectron.* 47 (2013) 545–552.
- D. Daems, K. Knez, F. Delpont, D. Spasic, J. Lammertyn, *Analyst* 141 (2016) 1906–1911.
- F. Canfarotta, A. Poma, A. Guerreiro, S. Piletsky, *Nat. Protoc.* 11 (2016) 443–455.
- M. V Sullivan, F. Allabush, H. Flynn, B. Balanethupathy, J.A. Reed, E.T. Barnes, C. Robson, P. O'Hara, L.J. Milburn, D. Bunka, *Glob. Challenges* (2023), 2200215.
- X. Yin, A.S. Hoffman, P.S. Stayton, *Biomacromolecules* 7 (2006) 1381–1385.
- B. Neises, W. Steglich, *Angew. Chem. Int. Ed. Engl.* 17 (1978) 522–524.
- C. Blackburn, H. Tai, M. Salerno, X. Wang, E. Hartsuiker, W. Wang, *Eur. Polym. J.* 120 (2019) 109259.
- C.J. Choi, B.T. Cunningham, *Lab Chip* 7 (2007) 550–556.
- B.R. Schudel, C.J. Choi, B.T. Cunningham, P.J.A. Kenis, *Lab Chip* 9 (2009) 1676–1680.
- M.F. Pineda, L.L.-Y. Chan, T. Kuhlenschmidt, C.J. Choi, M. Kuhlenschmidt, B. T. Cunningham, *IEEE Sensor. J.* 9 (2009) 470–477.
- H. Shafiee, E.A. Lidstone, M. Jahangir, F. Inci, E. Hanhauser, T.J. Henrich, D. R. Kuritzkes, B.T. Cunningham, U. Demirci, *Sci. Rep.* 4 (2014) 4116.
- Y. Chen, Q. Xie, X. Li, H. Zhou, X. Hong, Y. Geng, *J. Phys. D Appl. Phys.* 50 (2016), 25101.
- C. Liu, J. Wang, F. Wang, W. Su, L. Yang, J. Lv, G. Fu, X. Li, Q. Liu, T. Sun, *Opt Commun.* 464 (2020), 125496.
- S. Jain, K. Choudhary, S. Kumar, *Opt. Fiber Technol.* 73 (2022), 103030.
- J. Fan, L. Qiu, Y. Qiao, M. Xue, X. Dong, Z. Meng, *Front. Chem.* 9 (2021), 665119.

- [67] H. Wang, X. Wang, J. Wang, W. Fu, C. Yao, *Sci. Rep.* 6 (2016), 33140.
- [68] A. Poma, A. Guerreiro, M.J. Whitcombe, E. V Piletska, A.P.F. Turner, S.A. Piletsky, *Adv. Funct. Mater.* 23 (2013) 2821–2827.
- [69] M. V Sullivan, S.R. Dennison, J.M. Hayes, S.M. Reddy, *Biomed. Phys. Eng. Express* 7 (2021), 45025.
- [70] O. Kimhi, H. Bianco-Peled, *Langmuir* 23 (2007) 6329–6335.
- [71] E. Verheyen, J.P. Schillemans, M. Van Wijk, M.-A. Demeniex, W.E. Hennink, C. F. Van Nostrum, *Biomaterials* 32 (2011) 3008–3020.
- [72] M. Zayats, A.J. Brenner, P.C. Searson, *Biomaterials* 35 (2014) 8659–8668.
- [73] S. Timmermans, J. Souffriau, C. Libert, *Front. Immunol.* 10 (2019) 1545.